Chinese Chemical Letters 35 (2024) 108642

Contents lists available at ScienceDirect

Chinese Chemical Letters

journal homepage: www.elsevier.com/locate/cclet

Continuous microflow visible-light photocatalytic *N*-formylation of piperidine and its kinetic study

Yangyang Xu[a], Fang Zhao[a,*], Xuhong Guo[a,b,*]

[a] State Key Laboratory of Chemical Engineering, School of Chemical Engineering, East China University of Science and Technology, Shanghai 200237, China
[b] International Joint Research Center of Green Energy Chemical Engineering, Shanghai 200237, China

ARTICLE INFO

Article history:
Received 31 March 2023
Revised 22 May 2023
Accepted 31 May 2023
Available online 2 June 2023

Keywords:
Microflow
Visible-light photocatalysis
N-Formylation
Piperidine
Kinetics

ABSTRACT

N-formylation of amines, a class of synthetically important reactions, is typically conducted using metal catalysts that are relatively expensive or not readily available and usually needs harsh conditions to increase the reaction efficiency. Here, an efficient continuous microflow strategy was developed for the gas-liquid visible-light photocatalytic *N*-formylation of piperidine, which achieved a reaction yield of 82.97% and a selectivity of >99% at 12 min using cheap organic dye photocatalyst under mild reaction conditions. The influence of essential parameters, including light intensity, temperature and equivalents of the gas, additive and photocatalyst, on the reaction yield was systematically studied. Furthermore, kinetic investigations were conducted, exhibiting the dependence of reaction rate and equilibrium yield of *N*-formylpiperidine on light intensity, temperature and photocatalyst equivalent. The microflow photocatalytic approach established in this work, which realized a markedly higher space-time yield than the conventional batch method (37.9 *vs.* 0.212 mmol h^{-1} L^{-1}), paves the way for the continuous, green and efficient synthesis of *N*-formamides.

Formylation of amines is a synthetically significant reaction as *N*-formamides are valuable intermediates in the synthesis of pharmaceuticals, agrochemicals, dyes, *etc.* [1–5]. Formamides can act as Lewis base catalysts in hydrosilylation and alkylation of carbonyl compounds [6,7], and are also indispensable reagents in Vilsmeier formylation reactions [8].

In recent years, numerous methods have been reported on *N*-formylation of amines, which, however, usually require expensive metal catalysts and harsh reaction conditions such as high temperature and pressure [9–13]. The Glorius group [4] used methanol as the formylation reagent and Ru(cod)(2-methylallyl)$_2$ as the dehydrogenation catalyst for the formylation of primary and secondary amines at 125 °C. Chakraborty *et al.* [10] reported a method of using metal Mn complexes to catalyze amines and methanol to produce the corresponding formamides, where the reaction temperature was also high (110 °C), and the preparation of the catalyst was difficult and required strict anhydrous and oxygen-free environment. Therefore, it is still crucial to develop a green and efficient method with mild reaction conditions for formamide synthesis.

Over the past fifteen years, great progress has been made on photocatalysis, especially visible-light photocatalysis which has become one of the most powerful tools in organic synthesis [14–19]. Ghosh *et al.* reported the formylation of amines by visible-light photocatalysis, where *N*-formamides were generated from the reaction between the enamine intermediate and the oxygen in the air at room temperature under photocatalytic reactions [20]. However, the reaction was implemented in conventional glass vials where the gas-liquid mass transfer rate was very low due to the limited gas-liquid interfacial surface area and the light intensity distribution was inhomogeneous. As a result, the photocatalytic reaction rate in the glass vessels was largely limited and it still needed hours to complete the reaction in Ghosh's work.

The combination of photochemistry and flow chemistry has emerged as an enabling method in the past few years and can effectively resolve the above-described problems [21–30]. Especially, microflow photochemistry can achieve even illumination in the reaction mixture, and provide uniform and good gas-liquid dispersion, thereby imparting high interfacial area per unit volume to the gas-liquid mass transfer [31,32]. In this work, a continuous microflow photocatalytic strategy for the *N*-formylation of amines was developed. Using piperidine as the model substrate (Fig. 1a), the effects of various parameters, such as oxygen equivalent, operating pressure, light intensity, temperature, additive equivalent and

* Corresponding authors.
E-mail addresses: fzhao1@ecust.edu.cn (F. Zhao), guoxuhong@ecust.edu.cn (X. Guo).

https://doi.org/10.1016/j.cclet.2023.108642
1001-8417/

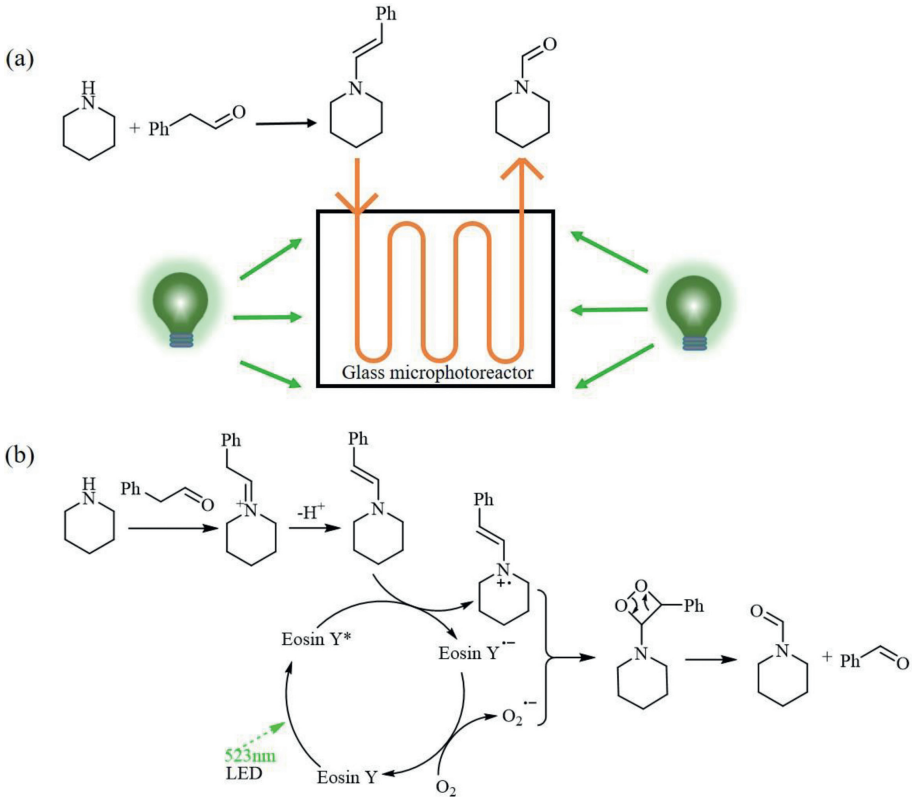

Fig. 1. (a) Schematics for the continuous microflow photocatalytic *N*-formylation of piperidine; (b) Proposed mechanism for the photocatalytic *N*-formylation of piperidine.

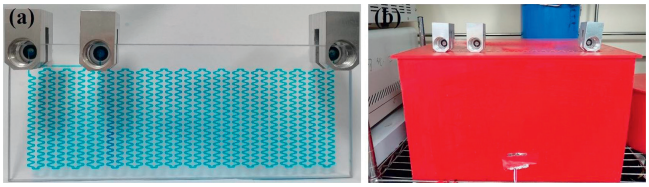

Fig. 2. (a) The glass microphotoreactor obtained by femtosecond laser engraving for the microflow photocatalytic synthesis of *N*-formamides in this work; (b) The photoreaction box custom-made by 3D printing to hold the light source and the microphotoreactor in this work.

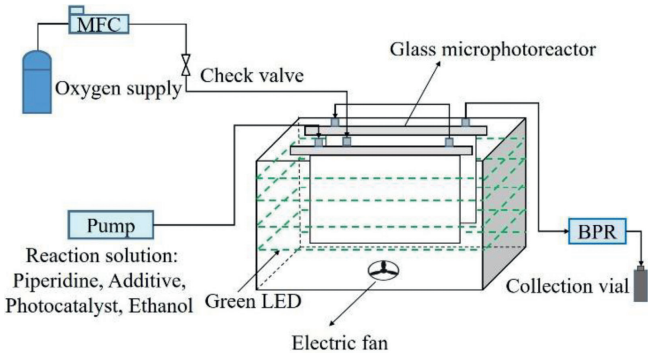

Fig. 3. Schematic diagram of the continuous microflow photocatalytic experimental setup. MFC and BPR represent mass flow controller and back pressure regulator respectively. The dashed lines represent the LED strips.

photocatalyst equivalent, on the reaction yield were systematically examined in continuous flow conditions. Furtherly, photocatalytic kinetic studies as well as the comparison between batch and continuous microflow methods were performed.

In order to enhance the gas-liquid dispersion and mass transfer in the visible-light photocatalytic *N*-formylation of amines, a glass microreactor (Fig. 2a) with special microchannel structures designed in our previous publication [33] was fabricated *via* femtosecond laser micromachining (see microreactor details in the Supporting information). As shown in Fig. 2b, two of the as-fabricated microphotoreactors (with a total internal volume of 6.348 mL) were connected in series and both installed in a red 3D-printed photoreaction box. Green LED stripes (maximum emission 523 nm) were wrapped around the interior vertical wall of the box. In order to reduce the illumination loss, aluminum foil was sticked onto the interior wall of the box prior to the LED strips. There was an observation hole with a detachable cover at the top of the box to facilitate the observation of fluid flow and dispersion in the microphotoreactor. Furthermore, some small ventilation holes, all having a Z-shape channel to reduce as many as possible photons that also went through the holes, were distributed properly on both the top and bottom of the box to facilitate heat dissipation. In addition, a small electric fan was fixed to the bottom of the box for cooling, and the temperature inside the photoreaction box was monitored by a thermocouple during the experiments.

Schematic representation of the experimental setup is shown in Fig. 3. The reaction solution consisting of piperidine, phenylacetaldehyde and Eosin Y disodium salt in ethanol was prepared and stirred in dark for at least 2 h to ensure the complete conversion of piperidine to the enamine intermediate. This liquid solution was fed to one of the two inlets of the microphotoreactor by a metering pump (2PB-1002IV-PT, SZWEICO). The oxygen gas was controlled by a mass flow controller (F-200CV-005-AGD-11-V, Bronkhorst) and entered the microphotoreactor *via* the other inlet. A back pressure regulator (HBP-1, HX-LOK) was connected at the outlet of the microphotoreactor. After the whole continuous microflow system reached a steady state, samples of the reaction

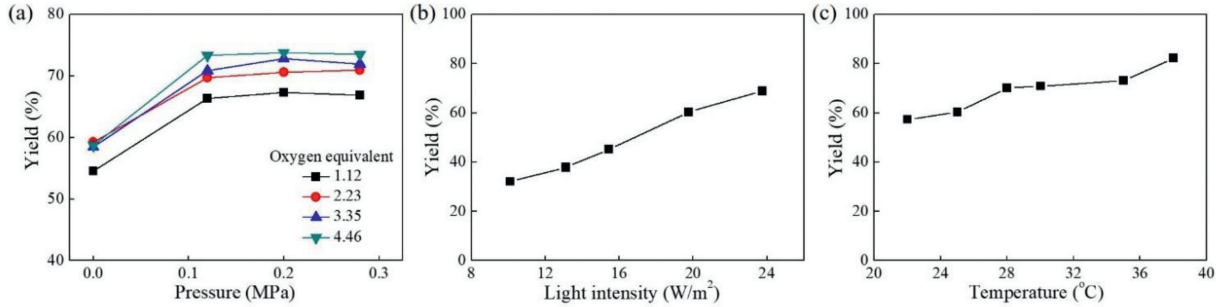

Fig. 4. (a) Effect of oxygen equivalent and operating pressure (gauge pressure) on the yield. (b) Effect of light intensity on the yield (liquid flow rate 1.058 mL/min, gas flow rate 0.794 mL/min, 30 °C, and 0.2 MPa). (c) Effect of temperature on the yield (liquid flow rate 0.529 mL/min, gas flow rate 0.397 mL/min, light intensity 19.75 W/m^2, and 0.2 MPa). Other conditions in the experiments of this figure: 10 mmol/L piperidine, 2 equiv. of phenylacetaldehyde, and 5 mol% Eosin Y disodium salt.

effluents were collected with light-tight vials. An internal standard (4-*tert*-butylcyclohexanone, 15 mg/mL) was added to the reaction mixture and the product yield was determined by GC/FID (GC-2014C, Shimadzu). The definition of the reaction yield is given by the following formula:

$$\text{Yield} = \frac{C_{1,p}}{C_0} \times 100\% \quad (1)$$

where $C_{1,p}$ and C_0 represent the concentration of *N*-formylpiperidine and the initial concentration of enamine respectively.

In the continuous microflow, precise control on the feeding ratio and uniform gas-liquid dispersion enable facile and accurate regulation of the gas amount for the reaction, which is difficult and sometimes impossible in batch. In this work, the oxygen equivalent was varied under different operating pressures in the continuous microflow photocatalytic set-up system, and the effects of oxygen equivalent and operating pressure on the yield of *N*-formylpiperidine were investigated. As shown in Fig. 4a, an increase in the oxygen equivalent from 1.12 to 4.46 resulted in higher yields when the operating pressure was fixed, which should be due to the fact that more superoxide radical anions were produced by molecular oxygen. Note that the improvement in the yield with the increasing of oxygen equivalent was not significant when the oxygen equivalent surpassed 3.35. In addition, when the operating pressure (gauge pressure) increased from 0 to 0.12 MPa, the yield increased evidently, while in the pressure range of 0.12 MPa to 0.28 MPa, the increase of pressure had no significant influence on the product yield.

Appropriate light intensity is crucial to obtain high yield and high selectivity for photoreactions. In this work, the change of light intensity was realized by changing the working current of the light source. From the proposed reaction mechanism in Fig. 1b [34–37], it can be seen that the increase of light intensity accelerates the formation of the excited state of the photocatalyst, which is then conducive to the subsequent generation of the radical cation of enamine and the superoxide radical anion. Consequently, it is not surprising that the photocatalytic yield in Fig. 4b increased evidently with the increase of light intensity.

Fig. 4c shows that an increase of the temperature resulted in the improvement of the reaction yield in the temperature range of 22-38 °C (the reaction temperature was varied by adjusting the power of the fan, and a thermocouple was fixed beside the glass microreactor in the photoreaction box to ensure the real-time monitoring of the temperature), indicating the effect of temperature on the photocatalytic formylation of piperidine could not be ignored. Higher temperatures can increase the chance that particles will collide, which in turn increase the reaction rate. For example, the frequency of collisions between the radical cation of enamine and the superoxide radical anion would increase at a high temperature, thereby producing more product molecules.

Then we investigated the effect of the equivalent of phenylacetaldehyde which acted as an additive on the yield of *N*-formylpiperidine. As is evident from Fig. 5a, the yield was elevated with the increase of the amount of phenylacetaldehyde used when the phenylacetaldehyde equivalent was less than 2. In the photocatalytic route shown in Fig. 1, phenylacetaldehyde was used to form enamine with piperidine before the microflow photocatalytic reaction. Fig. 5c shows the plausible reaction mechanism for the formation of enamine [38]. In order to understand the role of phenylacetaldehyde in this process, a simple kinetic study for the reaction between piperidine and phenylacetaldehyde was carried out (Fig. 5b). It can be seen that the increase of phenylacetaldehyde equivalent could increase the production rate of the enamine intermediate as well as the amount of the enamine produced. As a consequence, as the equivalent of phenylacetaldehyde rose during the formation of enamine, the yield of *N*-formylpiperidine in the subsequent photocatalytic reaction was improved. It can be also seen that the yield of *N*-formylpiperidine remained almost unchanged when the phenylacetaldehyde equivalent further increased beyond 2, implying that increasing the amount of phenylacetaldehyde no longer enhanced the enamine formation.

The presence of photocatalyst is vital for photocatalytic reactions. As shown in Fig. 6, the *N*-formylpiperidine yield rose distinctly from 43.80% to 72.11% by increasing the photocatalyst loading from 0.25 mol% to 2.5 mol%. However, a further increase of photocatalyst equivalent did not give rise to an improvement in yield. This could be potentially due to the limitations of photon transport and higher photon flux was required to achieve a higher yield at a higher photocatalyst usage.

Based on the above investigations on various parameters, we then carried out the microflow photocatalytic synthesis under optimized conditions (10 mmol/L piperidine, 2 equiv. of phenylacetaldehyde, 5 mol% Eosin Y disodium salt, liquid flow rate 0.529 mL/min, gas flow rate 0.397 mL/min, light intensity 23.74 W/m^2, 38 °C, and 0.2 MPa), and achieved a reaction yield of 82.97% and a selectivity of more than 99%.

Kinetic profiles for the microflow photocatalytic *N*-formylation of piperidine were attained under different light intensities, temperatures and photocatalyst loadings, respectively. Investigations on the elimination of gas-liquid mass transfer limitations were conducted ahead of time to ensure the subsequent reaction kinetics obtained was not affected by mass transfer (see details in Supporting information). As shown in Figs. 7a and b, when the light intensity or the temperature elevated, the reaction rate was accelerated evidently. Theoretically, the intrinsic kinetics of a photochemical reaction is determined by the photon flux and that of a thermal chemical reaction is determined by the temperature. And

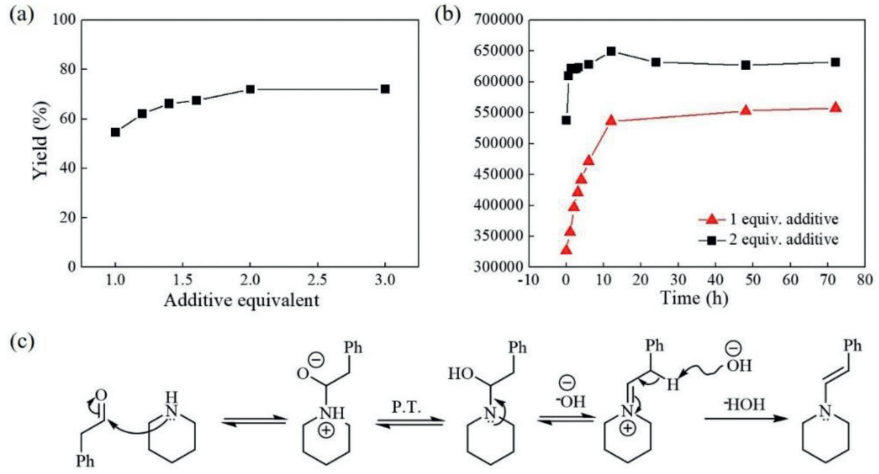

Fig. 5. (a) Effect of phenylacetaldehyde equivalent on the yield (10 mmol/L piperidine, 5 mol% Eosin Y disodium salt, liquid flow rate 0.529 mL/min, gas flow rate 0.397 mL/min, light intensity 19.75 W/m^2, 30 °C, and 0.2 MPa). (b) Kinetic curves for formation of enamine with 1 or 2 equiv. of phenylacetaldehyde respectively (10 mmol/L piperidine and 5 mol% Eosin Y disodium salt in batch). The vertical axis represents the GC peak area of enamine. (c) Plausible reaction mechanism for formation of enamine.

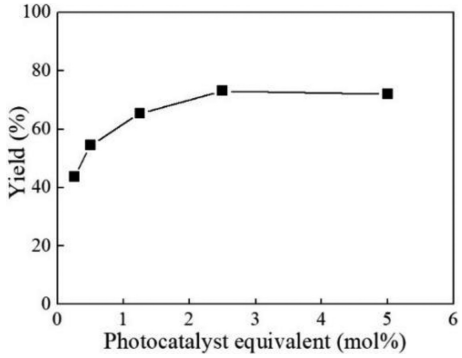

Fig. 6. Effect of photocatalyst equivalent on the yield (10 mmol/L piperidine, 2 equiv. of phenylacetaldehyde, liquid flow rate 0.529 mL/min, gas flow rate 0.397 mL/min, light intensity 19.75 W/m^2, 30 °C, and 0.2 MPa).

Table 1
Comparison of reaction results in batch and continuous microflow.[a]

	Reaction time (h)	Yield (%)	Selectivity (%)
Batch	24	81.20	82
Microflow	0.2	72.86	99

[a] Conditions: 10 mmol/L piperidine, 2 equiv. of phenylacetaldehyde, 5 mol% Eosin Y disodium salt, light intensity 19.75 W/m^2, 30 °C, and 0.2 MPa.

both the two types of the reactions are involved in the photocatalytic process to form *N*-formamides, as shown by the multi-step reaction mechanism in Fig. 1b, indicating that light intensity and temperature are both essential operating conditions that govern the reaction kinetics. Simultaneously, it is worth noting that increase in the light intensity did not change the final yield when the reaction was complete (*i.e.*, equilibrium yield), while the increase in the temperature could improve the equilibrium yield.

As expected, the increase of the photocatalyst equivalent would also increase the reaction rate greatly when the photocatalyst equivalent was below 2.5 mol% (Fig. 7c). Further increase of photocatalyst equivalent (>2.5 mol%) had no effect on the reaction rate due to the limitation of photon flux irradiating on reaction fluid.

Eventually, to validate the superiority of the protocol developed in this work, a comparison was conducted between continuous-flow and batch processing. A 10 mL flask connected with an oxygen balloon was used to investigate the photocatalytic *N*-formylation of piperidine in batch. In this reactor vessel, 6.348 mL (this volume is equal to the internal volume of the microphotoreactor used in the continuous-flow experiment) reaction solution was agitated with a magnetic stirrer and irradiated with the same light source adopted for the continuous-flow experiment. Table 1 shows comparison of reaction results between continuous microflow and batch under the same conditions of concentrations, temperature and light intensity. It can be seen that the reaction efficiency in the continuous-flow microreactor was remarkably higher than that in the batch vessel. It can be further calculated that the space-time yield in flow was two orders of magnitude higher than that in batch (37.9 *vs.* 0.212 mmol h^{-1} L^{-1}). The signif-

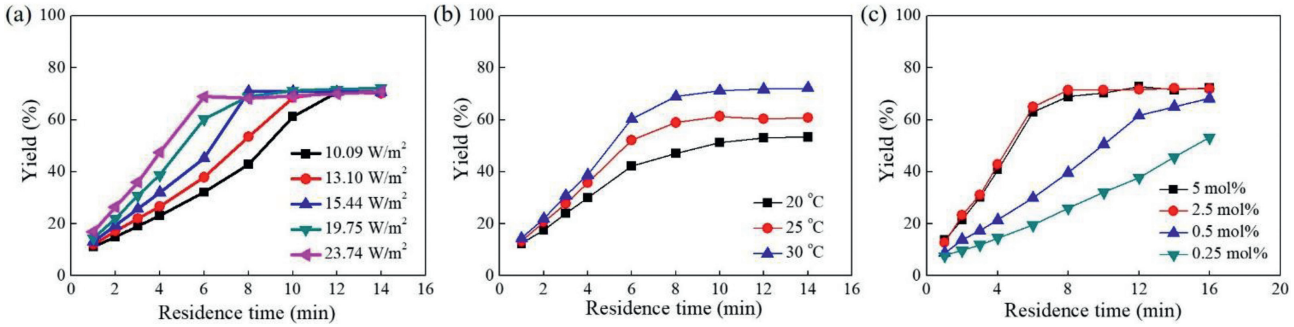

Fig. 7. (a) Reaction kinetics at various light intensities; (b) Reaction kinetics at various temperatures; (c) Reaction kinetics at various photocatalyst equivalents. Conditions in the kinetic experiments:10 mmol/L piperidine and 2 equiv. of phenylacetaldehyde.

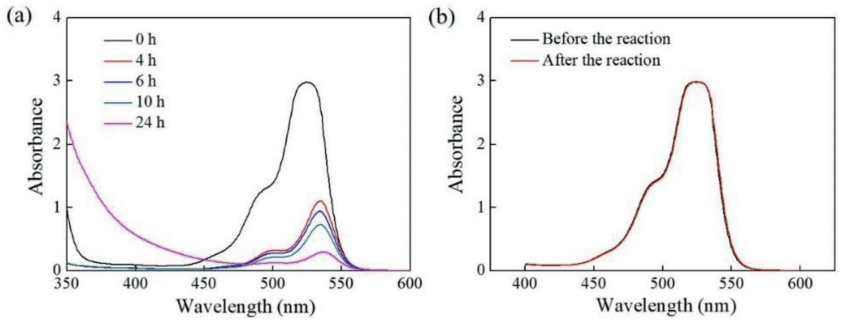

Fig. 8. (a) UV-vis absorption spectra of the reaction mixture at different reaction times in batch; (b) UV-vis absorption spectra of the reaction fluid before and after the reaction in continuous microflow.

icant acceleration of the reaction rate was mainly attributed to the enhanced mass transfer (especially gas- liquid mass transfer) and the good uniformity of light illumination in the self-designed and home-made microreactor in this work. The periodic expansion and contraction structures of the microreactor were capable of providing good mass transfer and enough residence time simultaneously at a relatively low pressure drop, which was highly suitable for the photocatalytic *N*-formylation in this work. Moreover, as is evident from Fig. 8a, severe photocatalyst degradation occurred during the photoreaction in batch, which could be probably attributed to the long reaction time and localized over-illumination in the batch reaction. In contrast, the UV-vis spectra (Fig. 8b) of the reaction fluid before and after the continuous microflow reaction confirmed that no obvious degradation of photocatalyst occurred. The results in Fig. 8 confirms that the microflow has the advantages of short reaction time and uniform illumination.

In the present study, a continuous microflow photoreaction set-up was constructed for the study of gas-liquid visible-light photocatalytic synthesis of *N*-formylpiperidine. The glass chip-microreactor made from femtosecond laser micromachining, the light source, and the cooling fan were all integrated in a light-tight and ventilated photoreaction box. Different reaction conditions such as oxygen equivalent, light intensity, and temperature were adjusted and screened accurately and efficiently, and reaction kinetics without the limitations of mass transfer was obtained in the microflow set-up. It was also demonstrated that the space-time yield of the flow method was two orders of magnitude higher than that of the batch method, indicating the findings of this work can offer an efficient strategy for the green synthesis of *N*-formamides.

Declaration of competing interest

The authors declare that they have no known competing financial interests or personal relationships that could have appeared to influence the work reported in this paper.

Acknowledgments

We gratefully thank the financial support from the National Natural Science Foundation of China (No. 21808059) and the Fundamental Research Funds for the Central Universities (No. JKA01221712).

Supplementary materials

Supplementary material associated with this article can be found, in the online version, at doi:10.1016/j.cclet.2023.108642.

References

[1] Z. Wu, Y. Zhai, W. Zhao, et al., Green Chem. 22 (2020) 737–741.
[2] M. Nasrollahzadeh, N. Motahharifar, M. Sajjadi, et al., Green Chem. 21 (2019) 5144–5167.
[3] J. Maity, A.H. Chowdhury, S.M. Islam, et al., Nanotechnology 31 (2020) 395605.
[4] N. Ortega, C. Richter, F. Glorius, Org. Lett. 15 (2013) 1776–1779.
[5] Y. Nishikawa, H. Nakamura, N. Ukai, et al., Tetrahedron Lett. 58 (2017) 860–863.
[6] S. Kobayashi, M. Yasuda, I. Hachiya, Chem. Lett. 5 (1996) 407–408.
[7] K. Iseki, S. Mizuno, Y. Kuroki, et al., Tetrahedron 55 (1999) 977–988.
[8] I.M. Downie, M.J. Earle, H. Heaney, et al., Tetrahedron 49 (1993) 4015–4034.
[9] P. Daw, S. Chakraborty, G. Leitus, et al., ACS Catal. 7 (2017) 2500–2504.
[10] S. Chakraborty, U. Gellrich, Y. Diskin-Posner, et al., Angew. Chem. Int. Ed. 56 (2017) 4229–4233.
[11] T.X. Zhao, G.W. Zhai, J. Liang, et al., Chem. Commun. 53 (2017) 8046–8049.
[12] W.F. Li, X.F. Wu, Chem. Eur. J. 21 (2015) 14943–14948.
[13] J.J. Zhang, W.T. Zhang, M.H. Xu, et al., J. Am. Chem. Soc. 140 (2018) 6656–6660.
[14] X. Wei, W. Boon, V. Hessel, et al., ACS Catal. 7 (2017) 7136–7140.
[15] C. Bottecchia, M. Rubens, S.B. Gunnoo, et al., Angew. Chem. Int. Ed. 56 (2017) 12702–12707.
[16] M.A. Cismesia, T.P. Yoon, Chem. Sci. 6 (2015) 5426–5434.
[17] A.A. Bartolomeu, R.C. Silva, T.J. Brocksom, et al., J. Org. Chem. 84 (2019) 10459–10471.
[18] A.V. Nyuchev, T. Wan, B. Cendon, et al., Beilstein J. Org. Chem. 16 (2020) 1305–1312.
[19] Y. Cheng, Y. Lin, J. Xu, et al., Appl. Surf. Sci. 366 (2016) 120–128.
[20] T. Ghosh, A. Das, B. Koenig, Org. Biomol. Chem. 15 (2017) 2536–2540.
[21] K. Wang, Y.C. Lu, J.H. Xu, et al., AIChE J. 52 (2006) 4207–4213.
[22] M. Al-Rawashdeh, F. Yue, N.G. Patil, et al., AIChE J. 60 (2014) 1941–1952.
[23] Y. Su, G. Chen, E.Y. Kenig, Lab Chip 15 (2014) 179–187.
[24] D.T. McQuade, P.H. Seeberger, J. Org. Chem. 78 (2013) 6384–6389.
[25] M. Oelgemoeller, Chem. Eng. Technol. 35 (2012) 1144–1152.
[26] Y. Su, N.J.W. Straathof, V. Hessel, et al., Chem. Eur. J. 20 (2014) 10562–10589.
[27] V. Hessel, D. Kralisch, N. Kockmann, et al., ChemSusChem 6 (2013) 746–789.
[28] J.P. Knowles, L.D. Elliott, K.I. Booker-Milburn, Beilstein J. Org. Chem. 8 (2012) 2025–2052.
[29] M.N. Kashid, A. Renken, L. Kiwi-Minsker, Chem. Eng. Sci. 66 (2011) 3876–3897.
[30] Y. Su, V. Hessel, T. Noël, AIChE J. 61 (2015) 2215–2227.
[31] M. Pasha, S. Liu, M. Shang, et al., Chem. Eng. J. 445 (2022) 136663.
[32] C. Shen, M. Shang, H. Zhang, et al., AIChE J. 66 (2020) 16841.
[33] W. Fan, F. Zhao, M. Chen, et al., Chin. J. Chem. Eng. 59 (2023) 85–91.
[34] J.S. DeHovitz, Y.Y. Loh, J.A. Kautzky, et al., Science 369 (2020) 1113–1118.
[35] G. Wu, Y. Li, X. Yu, et al., Adv. Synth. Catal. 359 (2016) 687–692.
[36] T.K.M. Akita, Chem. Lett. 2 (2009) 166–167.
[37] Z. Liang, J. Guo, P. Wang, et al., Chin. Chem. Lett. 34 (2023) 108001.
[38] G. Stork, A. Brizzolara, H. Landesman, et al., J. Am. Chem. Soc. 85 (1963) 207–222.